Analytica Chimica Acta xxx (xxxx) xxx

Contents lists available at ScienceDirect

Analytica Chimica Acta

journal homepage: www.elsevier.com/locate/aca

# One-pot ultrasonic synthesis of multifunctional Au nanoparticle-ferrocene-$WS_2$ nanosheet composite for the construction of an electrochemical biosensing platform

Guolin Hong [a, 1], Ruiting Chen [c, 1], Luyao Xu [c], Xing Lu [b], Zhenqing Yang [c], Guobao Zhou [b, **], Lei Li [b], Wei Chen [c, *], Huaping Peng [c, ***]

[a] Department of Laboratory Medicine, The First Affiliated Hospital of Xiamen University, Xiamen, 361003, People's Republic of China
[b] College of Biological, Chemical Sciences and Engineering, Jiaxing University, Jiaxing, 314001, People's Republic of China
[c] Department of Pharmaceutical Analysis, Faculty of Pharmacy, Fujian Medical University, Fuzhou, 350108, People's Republic of China

## HIGHLIGHTS

- One-pot ultrasonic process for preparing Multifunctional Au nanoparticles-ferrocene-$WS_2$ nanocomposite (AFW).
- AFW nanocomposite with enhanced electrochemical property was presented.
- Combining with the immune magnetic beads technology to develop immunosensing platform.
- A new avenue for design of $WS_2$ nanosheet based sensing platform.

## GRAPHICAL ABSTRACT

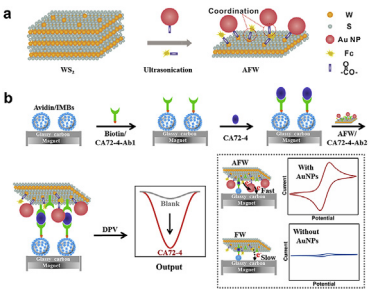


## ARTICLE INFO

*Article history:*
Received 29 September 2019
Received in revised form
4 November 2019
Accepted 16 November 2019
Available online xxx

*Keywords:*
Ultrasonic synthesis
$WS_2$ nanosheet
Au nanoparticle
Ferrocene monocarboxylic acid
Nanocomposite
Electrochemical biosensor

## ABSTRACT

Structuring of noble metal nanoparticles on transition metal dichalcogenide nanosheets induces significantly enhanced electronic, optical, and catalytic functions. However, the synthesis of multifunctional hybrids is always time-consuming and involves multiple steps. Herein, a ternary Au nanoparticle-ferrocene-$WS_2$ nanosheet (AFW) composite has been prepared by a facile one-step sonochemical approach. Stripped $WS_2$ nanosheets were functionalized with ferrocene monocarboxylic acid (FMC) and gold nanoparticles (AuNPs) by making use of the strong coordinative interaction of carboxyl groups with tungsten atoms. The AuNPs decorating the $WS_2$ nanosheet not only increase the water solubility of $WS_2$ nanosheet and surface area of the modified electrode, but also act as electron transport bridges to aid the tunneling of electrons from the small redox molecule, FMC, through the space to the electrode on which they are mounted. Furthermore, the ternary AFW nanocomposite could effectively avoid the leaching of FMC from the nanocomposite matrix and provided a suitable environment for the immobilized biomolecules. Combining the immune magnetic beads technology and the AFW nanocomposite with aforementioned advantages, a high-performance electrochemical immunosensor was successfully developed using carbohydrate antigen 72–4 (CA72-4) as a model analyte. A linear relationship in the range of 2–50 U/L for the detection of CA72-4 was found with a low detection limit of 0.6 U/L. In addition, the biosensor showed excellent performance in selectivity, stability, and reproducibility. Thus,

* Corresponding author.
** Corresponding author.
*** Corresponding author.
*E-mail addresses:* gbzhou@mail.zjxu.edu.cn (G. Zhou), chenandhu@163.com (W. Chen), penghuaping@fjmu.edu.cn (H. Peng).
[1] Guolin Hong and Ruiting Chen contributed equally to this work.

https://doi.org/10.1016/j.aca.2019.11.038

this work not only proposes a facile avenue for preparing a 2D $WS_2$ nanocomposite with multifunctional properties but also opens up a new method to extend the application of $WS_2$-based materials in biological sensing.



## 1. Introduction

Ultrathin transition metal dichalcogenide (TMD) nanosheets with unprecedented chemical, physical, electronic, and optical properties have attracted widespread interest in the last few decades [1–5]. TMDs, especially $MoS_2$ and $WS_2$ nanosheets epitaxial growthed or absorbed with noble metal nanoparticles and other inorganic materials have superior electronic and catalytic properties originating from exciton-plasmon coupling and unusual heterojunctions [6–8]. For example, $WS_2$ nanosheets coupled with tetragonal $WO_3$ nanoparticles facilitated the transport of excited electrons from the valence band to the conduction one, and promoted the separation of photo-generated electron-hole pairs, resulting in significantly enhanced photocatalytic activity [9]. In another study, Moshfegh et al. obtained a heterojunction nanocomposite of $WS_2$ nanosheets functionalized with CdS nanoparticles for enhanced photoelectrochemical water splitting [6]. Further, Huang et al. demonstrated the significantly improved performance of $WS_2$/Au hybrids in electrocatalytic hydrogen evolution reaction [7]. Kim et al. synthesized photocatalysts by decorating Pd nanoparticles on $WS_2$ nanosheets, to achieve extraordinary photocatalytic activity in Suzuki reactions [10].

Owing to the aforementioned excellent electrical and optical catalytic properties, 2D TMD nanosheets are being explored for potential application in the storage and generation of energy, such as hydrogen evolutions [11], supercapacitors [12], and lithium-ion batteries [13]. An upcoming trend in the field is the applications of TMD nanosheets in sensing nanodevices to take advantage of their marvellous surface-to-volume ratio, fluorescence, and rapid heterogeneous electron transport [2,14]. Zhang et al. illustrated that $MoS_2$ nanosheets could act as an efficient quencher of fluorescent dyes [14,15]. As a fluorophore-tagged single strand probe DNA interacts strongly with $MoS_2$ nanosheets, a DNA duplex formed by the target DNA and signal DNA was isolated from the $MoS_2$ nanosheets to recover the fluorescence of the dye. Jiang et al. fabricated a high performance biosensor for MicroRNA detection using $WS_2$ nanosheets as an efficient fluorescence quencher based on differential binding affinity toward short digested DNA fragment versus origin ssDNA sequence [16]. Moreover, monolayer $MoS_2$ was used to fabricate FET biosensors to reliably and ultrasensitively detect target DNA fragments [17]. Although many sensors and biosensors have been constructed, at present, the development of the sensors based on functional TMD nanosheet is limited by the multiple steps involved in their processing and modification.

Some of the common methods for fabricating thin layers of TMD nanosheets include mechanical cleavage, chemical vapor deposition, liquid-phase exfoliation, and lithium intercalation [18–21]. Among them, liquid-phase exfoliation is an easily operable low-cost technique. However, the poor water-solubility of layered TMD nanosheets produced in organic solvents strongly limits their applications in biosensing. Further modification of such TMD nanosheets by coating with polyethylene glycol (or polyacrylic acid) or intercalating with $Li^+$ ion is required to improve their solubility in water. Moreover, vapor-phase deposition methods and wet-chemical synthetic routes have been widely used to synthesize composites of noble metals and TMDs nanosheets. These epitaxial growth methods suffer from the shortcomings of low sensitivity and throughput to environmental conditions.

Similar to the method of the self-assembly of long-chain thiol polyethylene glycol on the surface of $WS_2$ [22], we herein proposed a one-pot way for the synthesis of a ternary Au nanoparticle (AuNP)-ferrocene-$WS_2$ (AFW) hybrid by exploiting the coordinative interaction between the carboxyl groups and tungsten atoms [23]. AuNPs and ferrocene monocarboxylic acid (FMC) could self-assemble on layered $WS_2$ nanosheets during their exfoliation through liquid-phase sonication. AuNPs with high biocompatibility have been widely applied in various biosensing nanodevices. Combination of the great surface area of $WS_2$ nanosheets, abundant AuNPs were assembled on them to further improve their electronic property as well as water solubility, which led to significant improvement electron transport from FMC to the electrode. As the self-assembled small redox molecule, FMC, can produce a considerable electrochemical signal, we employed the functionalized AFW nanocomposite to construct an immunosensor analysis platform. By combining our multi-functional probe with the immune magnetic bead (IMB) technology, we achieved highly sensitive biosensing of carbohydrate antigen 72–4 (CA72-4), thus extending the application field of metal nanoparticle-functionalized $WS_2$ nanosheets to biological sensing.

## 2. Experimental section

### 2.1. Materials and reagents

FMC, bulk $WS_2$, and bovine serum albumin (BSA) were purchased from Sigma (USA). Streptavidin-coated immune magnetic beads (Avidin-IMB), carbohydrate antigen 72–4 (CA72-4), biotinylated monoclonal anti-CA72-4 antibody (CC49, mouse), and monoclonal anti-CA72-4 antibody (B72.3, mouse) were purchased from Roche Diagnostics Ltd. (Switzerland). Phosphate buffer solutions (PBS, 0.1 M) containing 0.1 M KCl was used as the electrolyte.

### 2.2. Characterization

Electrochemical experiments were all recorded on an electrochemical workstation (Autolab PGSTAT30) with the typical three-electrode system: a modified glassy carbon electrode (GCE) as the working electrode, a platinum wire as the counter electrode, and an Ag/AgCl electrode as the reference electrode. Electrochemical impedance spectra (EIS) were recorded at 210 mV in the frequency range of $10^{-2}$ to $10^5$ Hz. The amplitude of the applied sine wave potential was 5 mV. Transmission electron microscopy (TEM) and Energy dispersive X-ray (EDX) spectrometry were characterized by JEOL 2010 (Japan). UV–vis absorption spectra were performed on UV-2450 spectrophotometer (Shimadzu).

### 2.3. Preparation of AuNP-FMC-$WS_2$ nanocomposite

Au NPs were synthesized by the reported method [24]. For the synthesis of the nanocomposite, 100 mg of $WS_2$, 4 mL of Au NP suspension, and 50 mg of FMC were mixed in 20 mL of Q-$H_2O$ and ultrasonically treated for 6 h. The mixture was centrifuged at

Please cite this article as: G. Hong et al., One-pot ultrasonic synthesis of multifunctional Au nanoparticle-ferrocene-$WS_2$ nanosheet composite for the construction of an electrochemical biosensing platform, Analytica Chimica Acta, https://doi.org/10.1016/j.aca.2019.11.038

10,000 rpm (10 min), and the supernatant was then centrifuged at 16,000 rpm (10 min). The precipitated final product of AFW nanocomposite was collected and washed with $H_2O/C_2H_5OH$ (v/v, 1:1). It was then re-suspended in Q-water (1 mL). In addition, FMC-$WS_2$ complex was prepared without the AuNPs following a similar procedure.

### 2.4. Preparation of AFW/CA72-4-Ab2

1 mL of 6 μg/mL CA72-4-Ab2 was added to the AFW (1 mL) under reflux at 37 °C for 20 min. Subsequently, BSA solution (50 μL, 100 mg/mL) was mixed with the above solution to block the AFW for 1 h with gentle stirring. The mixture was centrifuged (16000 rpm) and rinsed with 1 mL of PBS containing 0.5% BSA (pH 7.4). The centrifuge/wash steps were repeated thrice to remove excess CA72-4-Ab2. The final AFW/CA72-4-Ab2 was suspended in PBS (1 mL, pH 7.4) and stored at 4 °C until further use.

### 2.5. Fabrication of the immunosensor

A GCE was polished with alumina slurries (1.0, 0.3, and 0.05 μm, sequentially) and then ultrasonically washed in $HNO_3/H_2O$ (v/v, 1:1), $C_2H_5OH$, and water, each for 3 min, respectively. After being dried by $N_2$, 10 μL of avidin-modified IMB suspension was dripped onto the cleaned GCE surface and dried in a vacuum environment at room temperature. Next, 10 μL of biotin-modified CA72-4-Ab1 was immobilized on the above electrode and incubated at room temperature. The recognition probe, CA72-4-Ab1 was modified on the GCE surface through avidin-biotin interaction. After further incubated in a BSA solution (10%) for 30 min at room temperature to avoid nonspecific adsorption, the immunosensor was rising with PBS (pH 7.4) and stored at 4 °C before further used for CA72-4 detection.

### 2.6. Measurement procedure

10 μL of the CA72-4 standard solution (concentrations range from 0 to 1000 U/L) was incubated with the immunosensor for 1 h at 37 °C. Then, 10 μL of the AFW/CA72-4-Ab2 nanocomposite suspension was incubated with the above sensing interface for another 1 h. After it was rewashed with PBS, differential pulse voltammetry (DPV) was performed to record the peak current of FMC deposited on the immunosensor (0.1 M PBS, pH 7.4). DPV was performed from −0.6 to 0.3 V with pulse amplitude of 25 mV for the quantitative analysis of CA72-4.

## 3. Results and discussion

### 3.1. Mechanism of the operation of the proposed biosensor

The ternary AuNP-FMC-$WS_2$ nanocomposite was synthesized through a single-step sonication procedure (Scheme 1a). The bulk $WS_2$ solid material was split into single- and multi-layer structures through sonication in the presence of Au NPs and FMC in water. AuNPs prepared through citrate reduction, and the redox molecule FMC were self-assembled on $WS_2$ nanosheets to form the AFW hybrid through coordinative interaction between the carboxyl group of FMC and the unsaturated W atom at the margin of $WS_2$ nanosheets. The principle of the operation of the AFW nanocomposite used as a signal probe in the construction of the electrochemical sandwich biosensor is depicted in Scheme 1b. Avidin-IMBs were first immobilized on the GCE surface for immobilization

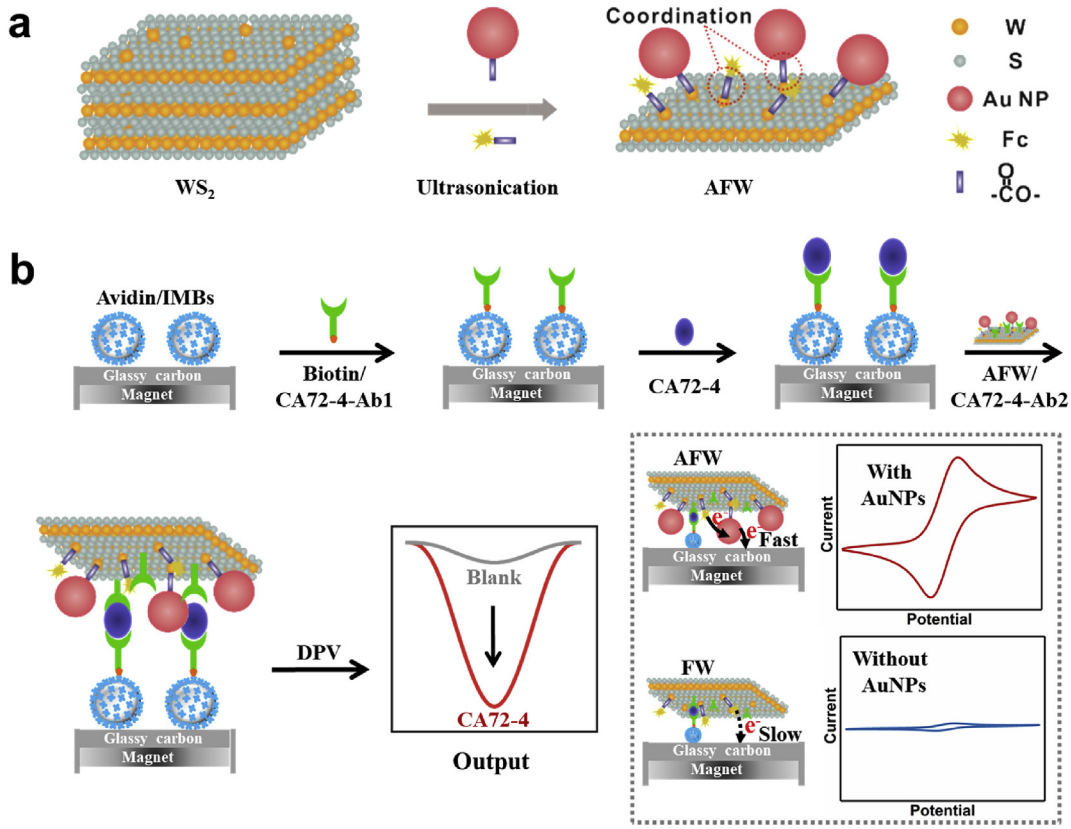


**Scheme 1.** (a) Schematic representation of the synthesis of the AFW nanocomposite. (b) Schematic illustration of the electrochemical immunosensor.

Please cite this article as: G. Hong et al., One-pot ultrasonic synthesis of multifunctional Au nanoparticle-ferrocene-$WS_2$ nanosheet composite for the construction of an electrochemical biosensing platform, Analytica Chimica Acta, https://doi.org/10.1016/j.aca.2019.11.038

of CA72-4-Ab1 through avidin-biotin covalent binding. The immunoreaction between the antibody and antigen could occur in the presence of the analyte, CA72-4. Then, CA72-4-Ab2-modified AFW nanocomposite could further bind to the immunoelectrode and act as a signal tag. The layered $WS_2$ nanosheets with high surface area and abundant quantity of FMC were explored as a signal probe, to significantly improve the sensitivity of the biosensor. In addition, an abundance of Au NPs loaded on $WS_2$ nanosheets could further remarkably enhance the electronic conductivity of FMC because metal NPs can help the redox molecule FMC to tunnel electrons through the space onto the electrode interface. The corresponding electrochemical DPV current generated by FMC was measured to quantify the concentration of CA72-4.

### 3.2. Characterization of the AFW nanocomposite

$WS_2$ nanosheets were prepared as reported previously [23]. AuNPs and FMC were decorated on $WS_2$ nanosheets through a one-pot sonication procedure for the first time. The surface morphology of the AFW nanocomposites was then characterized by TEM. As shown in Fig. 1A–C, massive layered $WS_2$ was stripped into one or few-layered structure with a large surface area, upon which a large number of AuNPs and FMC could be loaded through self-assembly. The $WS_2$ nanosheets were uniformly decorated with AuNPs. Notably, the 2D FMC-$WS_2$ nanosheet composite without AuNPs could also be prepared by the proposed one-pot sonication approach. Since the small FMC molecule could not be seen by TEM, EDX spectroscopy was characterized to identify the chemical composition of the AFW nanocomposite (Fig. 1D and E). Elemental peaks observed for W, Fe, and Au clearly demonstrate the successful self-assembly of FMC and AuNPs on $WS_2$ nanosheets.

The formation of the AFW nanocomposite was further confirmed by UV–vis absorption spectroscopy. Fig. 2 shows the UV–vis absorption spectra of FMC, FMC-$WS_2$ nanocomposite, AuNPs, and AFW nanocomposite. The absorption peak corresponding the FMC at 260 nm [25] and the Au plasmon band at 550 nm [26] in the UV–vis spectrum of the AFW nanocomposite together suggested the decoration of AuNPs and FMC on the surface of $WS_2$ nanosheets.

In this study, the AFW nanocomposite with a large signal probe loading centers and enhanced water solubility or stability met all the prerequisites for a biosensor system. The electrochemical response of the AFW was investigated according to the redox activity of FMC. Fig. 3 shows the CV curves of bulk $WS_2$, FMC-$WS_2$ nanocomposite, and AFW nanocomposite. No redox peaks were observed for the bulk $WS_2$-modified GCE, whereas a pair of well-outlined CV peaks of the FMC-$WS_2$ nanocomposite-modified electrode were located at +332 and + 379 mV, respectively (blue line), which is owe to the redox reaction of the FMC moiety in the nanocomposite. Furthermore, previous studies have shown that the AuNP acts as a mediator for the tunneling of electrons, closer to the GCE surface. Similarly, AuNPs could accelerate the electron convey of redox FMC molecule on electrode surface. On the other hand, the surface area of the modified electrode could be effectively increased after modification of AuNPs on $WS_2$ sheets, so that increasing the number of ferrocene molecules on AFW composite. Thus, significantly enhanced CV response of the electrode with using AFW has been achieved due to the increased surface area and accelerated electron transfer rate.

### 3.3. Electrochemical characterization of the immunosensor

The CV and AC impedance characteristics of the sandwich biosensor obtained by the step-by-step assembly processes were investigated. Fig. 4A shows the CV curves for the bare GCE, IBM-modified GCE, CA72-4-Ab1/IBM/GCE, CA72-4/CA72-4-Ab1/IBM/GCE, and AFW-CA72-4-Ab2/CA72-4/CA72-4-Ab1/IBM/GCE. The bare GCE (curve a) shows good reversibility with a peak-to-peak separation $\Delta E_p$, while the electrode modified in a stepwise fashion (curve b-e) exhibits a slightly irreversible response with enlarged $\Delta E_p$. This can be attributed to the stepwise assembly of the

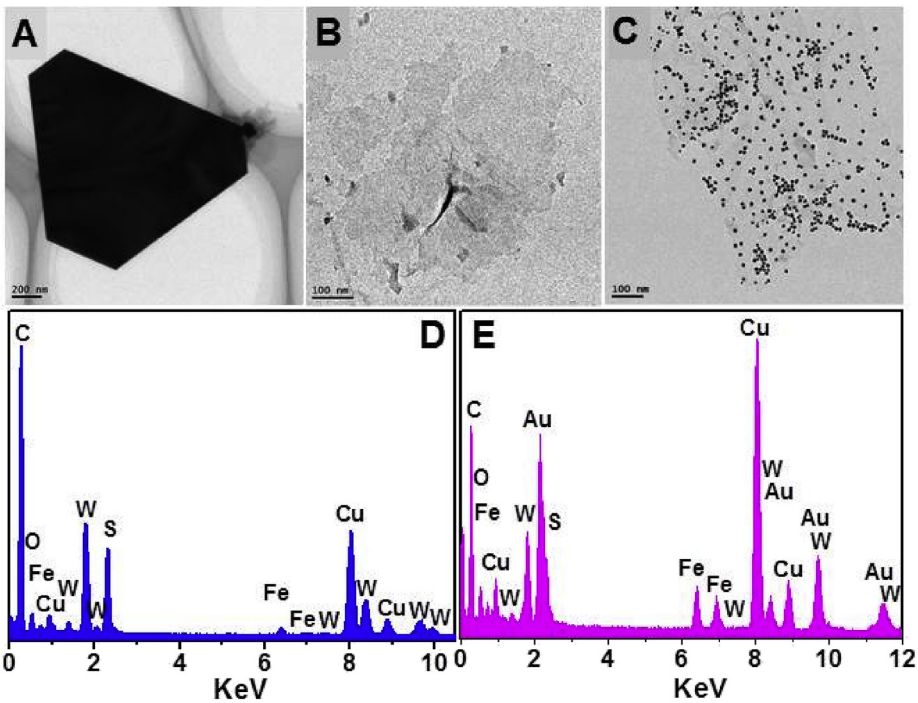


**Fig. 1.** TEM images of bulk $WS_2$ (A), FMC-$WS_2$ nanocomposite (B), and AFW nanocomposite (C). EDX spectra of FMC-$WS_2$ nanocomposite (D) and AFW nanocomposite (E).

Please cite this article as: G. Hong et al., One-pot ultrasonic synthesis of multifunctional Au nanoparticle-ferrocene-$WS_2$ nanosheet composite for the construction of an electrochemical biosensing platform, Analytica Chimica Acta, https://doi.org/10.1016/j.aca.2019.11.038

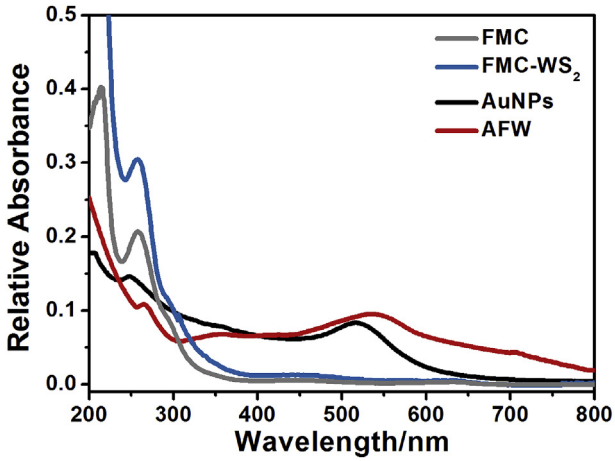


**Fig. 2.** UV–vis absorption spectra of FMC (gray line), FMC-$WS_2$ nanocomposite (blue line), AuNPs (black line) and AFW nanocomposite (red line). (For interpretation of the references to colour in this figure legend, the reader is referred to the Web version of this article.)

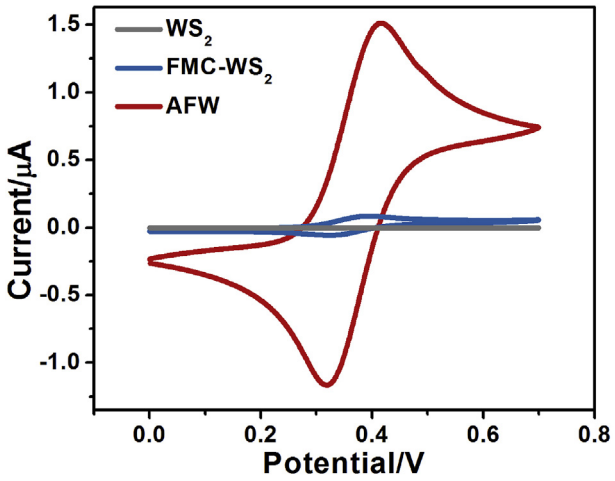


**Fig. 3.** CVs of bulk $WS_2$ (gray), FMC-$WS_2$ nanocomposite (blue), and AFW nanocomposite (red). (For interpretation of the references to colour in this figure legend, the reader is referred to the Web version of this article.)

biomolecules and biomaterials on the GCE, which reduced the rate of electron transfer. Accordingly, as shown in Fig. 4B, the bare GCE shows negligible impedance (curve a), indicating its good electrical conductivity. After the avidin-modified IBMs were loaded onto the GCE, they induced an increase in the electrochemical impedance (curve b). When biotin-CA72-4-Ab1 was modified onto the GCE, the impedance increased again owing to the binding of biotin-CA72-4-Ab1 to avidin-IBMs (curve c). Upon the addition of the target antigen, CA72-4, the antibody-antigen immunoreaction resulted in a further increase in the electrochemical impedance (curve d). After the AFW-CA72-4-Ab2 was captured by the modified GCE, the formation of immunological recognition complex led to a significant improvement in the resistance of the working electrode interface (curve e). These results successfully validate the achievement of an immunoreaction-based biomolecule recognition interface.

### 3.4. Optimization of measurement variables

In order to carry out the best performance of the constructed biosensor, the effects of incubation pH, incubation time, and

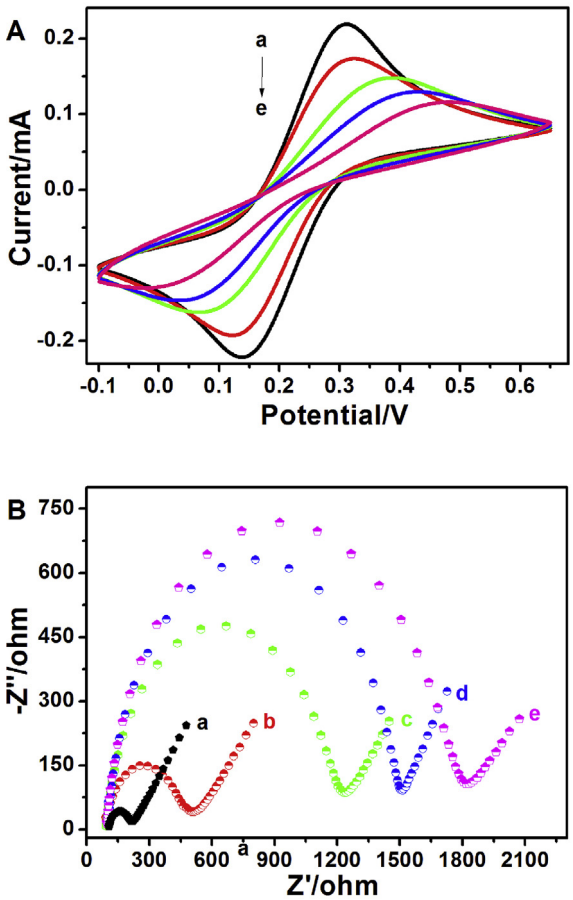


**Fig. 4.** CVs (A) and EIS (B) of the different electrodes in 5 mmol/L $[Fe(CN)_6]^{3-/4-}$. (a) Bare GCE, (b) IBM/GCE, (c) CA72-4-Ab1/IBM/GCE, (d) CA72-4/CA72-4-Ab1/IBM/GCE, (e) AFW-CA72-4-Ab2/CA72-4/CA72-4-Ab1/IBM/GCE.

incubation temperature of AFW-CA72-4-Ab2 on the behavior of the immunosensor were optimized. Results shown in Fig. 5 indicated that a pH of 7.4, incubation time of 25 min, and immunoreaction at 30 °C could result in the best signal from the biosensing platform. Thus, these conditions were selected as optimized parameters for further CA72-4 detection.

### 3.5. Analytical performance towards CA72-4

Under the optimal experiment conditions, the sensitivity of the immunosensor in antigen analysis was finally investigated. Fig. 6A shows the DPV current response with the addition of a range of CA72-4 solutions with varying concentrations. As shown, the peak current of DPV improved gradually with increasing CA72-4 concentration. Fig. 6B shows a good linear relationship between the DPV peak current and the logarithm value of the CA72-4 concentration in the range of 2–50 U/L. The linear regression equation is expressed as, $\Delta I_{peak} = -1.08-0.02\lg C$ (U/L). The sensing platform showed a good sensitivity with a detection limit of 0.6 U/L (S/N = 3). The detection limit of the biosensor for CA72-4 is comparable to or better than those of some of the previously reported sensors [27–30]. The excellent detection sensitivity can be attributed to $WS_2$ nanosheets containing large amounts of the redox molecule FMC and AuNPs, which greatly accelerated the electron transport between the FMC and electrode.

Please cite this article as: G. Hong et al., One-pot ultrasonic synthesis of multifunctional Au nanoparticle-ferrocene-$WS_2$ nanosheet composite for the construction of an electrochemical biosensing platform, Analytica Chimica Acta, https://doi.org/10.1016/j.aca.2019.11.038

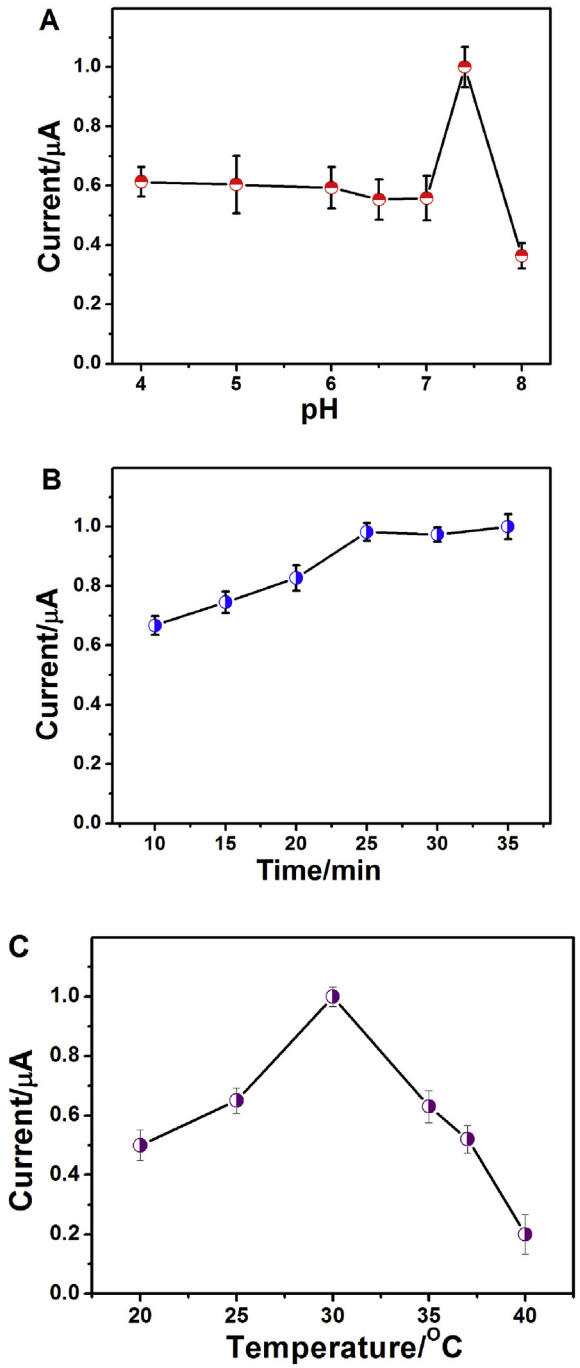


**Fig. 5.** The effects of AFW-Ab2 incubation pH (A), incubation time (B), and incubation temperature (C) on the response of the immunosensor.

### 3.6. Selectivity, reproducibility, and stability studies

Selectivity is one of the important characteristics of an immunosensor. Possible interfering antigens were used to evaluate the selectivity of the immunosensor. The immunosensors were incubated in 20 U/L of CA72-4, 20 U/mL of carcinoma antigen 199 (CA199), 200 ng/mL of carcinoembryonic antigen (CEA) and prostate-specific antigen (PSA), respectively. The recorded DPV peak currents of the redox couple of FMC are −1.43 μA for CA72-4, −0.96 μA for CA199, −0.99 μA for CEA, and −0.98 μA for PSA, indicating that these interfering antigens at relatively high

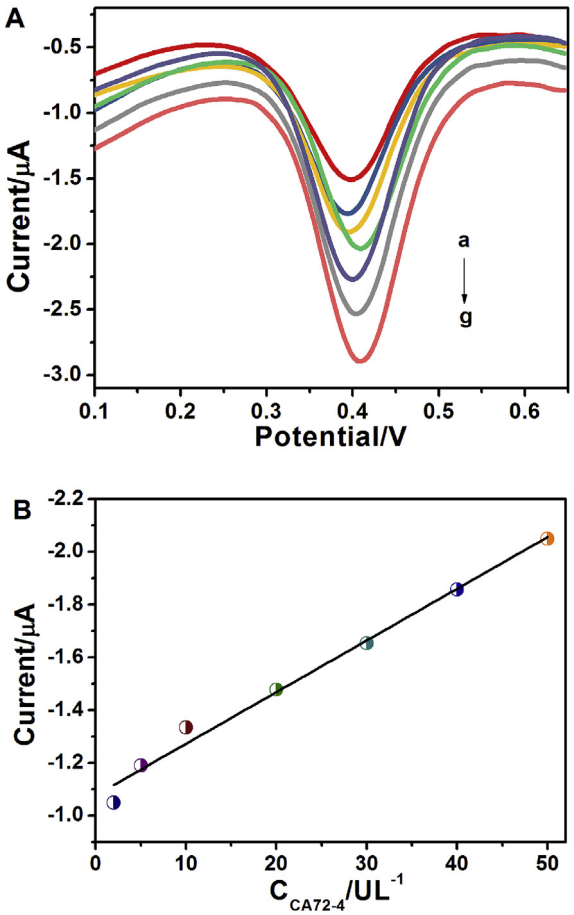


**Fig. 6.** DPV responses of the immunosensor toward varied concentrations of (A) CA72-4 and the (B) calibration curve constructed using the CA72-4 analysis strategy. Curves a-g corresponding to CA72-4 concentration in the range of 2−50 U/L.

concentrations did not affect the CA72-4 detection capability. To further confirm the selectivity of the immunosensor, the sensors were incubated with CA72-4 respectively containing CA199, CEA and PSA, no remarkable difference in the DPV peak current of the system was observed as compared to that of the pure CA72-4 system, demonstrating the good selectivity of the immunoassay.

To evaluate the reproducibility of the immunosensor response, 6 electrodes were prepared for the detection of 20 U/L of CA72-4. The relative standard deviation (RSD) of the results of measurements on the 6 electrodes is 3.9%, which indicates acceptable reproducibility. The storage stability of the immunosensor was also investigated. When not in use, the electrodes were stored in PBS at 4 °C. After two weeks, the immunosensor retained ~90% of its initial response. This good stability is possibly due to the excellent AFW composite film which prevented the leaching of both FMC and antibodies, and retained the activity of antibodies effectively.

### 3.7. Application of the immunosensor towards the detection of CA72-4

In order to evaluate the feasibility of using the immunosensor for real sample analysis, the immunosensor was used for the detection of CA72-4 in human serum samples by the standard addition method. It shows an acceptable recovery in the range of 92.7−108% with an RSD of 1.3−4.7%, indicating that the present immunosensor might provide a feasible alternative method for detecting CA72-4 in human serum samples.

Please cite this article as: G. Hong et al., One-pot ultrasonic synthesis of multifunctional Au nanoparticle-ferrocene-$WS_2$ nanosheet composite for the construction of an electrochemical biosensing platform, Analytica Chimica Acta, https://doi.org/10.1016/j.aca.2019.11.038

## 4. Conclusions

A facile one-pot sonication method has been proposed to synthesize a 2D-$WS_2$ based nanocomposite with multifunctional properties. Herein, a redox mediator, FMC, and functional AuNPs were decorated on $WS_2$ nanosheets by simple self-assembly utilizing the strong coordination interaction between the carboxyl groups and tungsten atoms at the edge of $WS_2$ nanosheets under sonolysis treatment. The multifunctional AFW nanocomposite was then applied to construct a highly sensitive immunobiosensing platform. The AFW nanocomposite not only provided a beneficial microenvironment to maintain the binding affinity of proteins, but also enlarged the loading capacity of FMC and biomolecules and enhanced the conductivity and charge-transport properties of the composites. Furthermore, the AFW could eliminate the leaching of FMC from the matrix and thus retained its electrochemical property. With the above merits, the constructed electrochemical immunobiosensor with simple, stable, and sensitive properties has potential for application in medical diagnosis. Therefore, this work develops a facile approach for the preparation of a $WS_2$ nanocomposite with multifunctional properties and their great potential applications in other fields.

## Author contribution statement

Guolin Hong: Conceptualization, Data curation, Writing- Original draft preparation. Ruiting Chen: Data curation, Writing- Original draft preparation. Luyao Xu: Methodology, Software. Xing Lu: Software, Validation. Zhenqing Yang: Data curation. Guobao Zhou: Writing- Reviewing and Editing. Lei Li: Software, Validation. Wei Chen: Supervision, Conceptualization. Huaping Peng: Project administration, Writing- Reviewing and Editing.

## Declaration of competing interest

The authors declare that they have no known competing financial interests or personal relationships that could have appeared to influence the work reported in this paper.

## Acknowledgements

This work was supported by the National Natural Science Foundation of China (NSFC Grants 21677060 and 21874020); Fujian Province Young Talent Supporting Project, China (2019B016); the Zhejiang Provincial Natural Science Foundation of China (Grants LQ19B050002); the Natural Science Foundation of Fujian Province, China (2019J01305, 2016J05031); Fujian Province Health Commission Young and Middle-Aged Talent training project, China (Grant No. 2018-ZQN-62) and Program for Fujian Youth Talent Support Project, China (2019B016).

## Appendix A. Supplementary data

Supplementary data to this article can be found online at https://doi.org/10.1016/j.aca.2019.11.038.

## References

[1] S. Karunakaran, S. Pandit, B. Basu, M. De, Simultaneous exfoliation and functionalization of 2H-$MoS_2$ by thiolated surfactants: applications in enhanced antibacterial activity, J. Am. Chem. Soc. 140 (2018) 12634–12644.

[2] C. Tan, X. Cao, X.J. Wu, Q. He, J. Yang, X. Zhang, J. Chen, W. Zhao, S. Han, G.H. Nam, M. Sindoro, H. Zhang, Recent advances in ultrathin two-dimensional nanomaterials, Chem. Rev. 117 (2017) 6225–6331.

[3] K. Yang, J.C. Blancon, W. Jiang, H. Zhang, J. Wong, E. Yan, Y.R. Lin, J. Crochet, M.G. Kanatzidis, D. Jariwala, T. Low, A.D. Mohite, H.A. Atwater, Giant enhancement of photoluminescence emission in $WS_2$-two-dimensional perovskite heterostructures, Nano Lett. 19 (2019) 4852–4860.

[4] Y. Chen, C. Tan, H. Zhang, L. Wang, Two-dimensional graphene analogues for biomedical applications, Chem. Soc. Rev. 44 (2015) 2681–2701.

[5] H.P. Peng, P. Liu, W.H. Wu, W. Chen, X.Y. Meng, X.H. Lin, A.L. Liu, Facile electrochemiluminescence sensing platform based on water-soluble tungsten oxide quantum dots for ultrasensitive detection of dopamine released by cells, Anal. Chim. Acta 1065 (2019) 21–28.

[6] M. Zirak, M. Zhao, O. Moradlou, M. Samadi, N. Sarikhani, Q. Wang, H.L. Zhang, A.Z. Moshfegh, Controlled engineering of $WS_2$ nanosheets–CdS nanoparticle heterojunction with enhanced photoelectrochemical activity, Sol. Energy Mater. Sol. Cells 141 (2015) 260–269.

[7] J. Kim, S. Byun, A.J. Smith, J. Yu, J. Huang, Enhanced electrocatalytic properties of transition-metal dichalcogenides sheets by spontaneous gold nanoparticle decoration, J. Phys. Chem. Lett. 4 (2013) 1227–1232.

[8] X. Huang, Z. Zeng, S. Bao, M. Wang, X. Qi, Z. Fan, H. Zhang, Solution-phase epitaxial growth of noble metal nanostructures on dispersible single-layer molybdenum disulfide nanosheets, Nat. Commun. 4 (2013) 1444.

[9] N. Huo, Q. Yue, J. Yang, S. Yang, J. Li, Abnormal photocurrent response and enhanced photocatalytic activity induced by charge transfer between $WS_2$ nanosheets and $WO_3$ Nanoparticles, ChemPhysChem 14 (2013) 4069–4073.

[10] F. Raza, D. Yim, J.H. Park, H.I. Kim, S.J. Jeon, J.H. Kim, Structuring Pd nanoparticles on 2H-$WS_2$ nanosheets induces excellent photocatalytic activity for cross-coupling reactions under visible light, J. Am. Chem. Soc. 139 (2017) 14767–14774.

[11] G. Sun, J. Liu, X. Zhang, X. Wang, H. Li, Y. Yu, W. Huang, H. Zhang, P. Chen, Fabrication of ultralong hybrid microfibers from nanosheets of reduced graphene oxide and transition-metal dichalcogenides and their application as supercapacitors, Angew. Chem. Int. Ed. 53 (2014) 12576–12580.

[12] Y. Wang, L. Yu, X.W. Lou, Synthesis of highly uniform molybdenum–glycerate spheres and their conversion into hierarchical $MoS_2$ hollow nanospheres for lithium-ion batteries, Angew. Chem. Int. Ed. 55 (2016) 7423–7426.

[13] G. Yang, C. Zhu, D. Du, J. Zhu, Y. Lin, Graphene-like two-dimensional layered nanomaterials: applications in biosensors and nanomedicine, Nanoscale 7 (2015) 14217–14231.

[14] Y. Zhang, B. Zheng, C. Zhu, X. Zhang, C. Tan, H. Li, B. Chen, J. Yang, J. Chen, Y. Huang, L. Wang, H. Zhang, Single-layer transition metal dichalcogenide nanosheet-based nanosensors for rapid, sensitive, and multiplexed detection of DNA, Adv. Mater. 27 (2015) 935–939.

[15] C.F. Zhu, Z.Y. Zeng, H. Li, F. Li, C.H. Fan, H. Zhang, Single-layer $MoS_2$-based nanoprobes for homogeneous detection of biomolecules, J. Am. Chem. Soc. 135 (2013) 5998–6001.

[16] Q. Xi, D.M. Zhou, Y.Y. Kan, J. Ge, Z.K. Wu, R.Q. Yu, J.H. Jiang, Highly sensitive and selective strategy for microrna detection based on $WS_2$ nanosheet mediated fluorescence quenching and duplex-specific nuclease signal amplification, Anal. Chem. 86 (2014) 1361–1365.

[17] J. Liu, X. Chen, Q. Wang, M. Xiao, D. Zhong, W. Sun, G. Zhang, Z. Zhang, Ultrasensitive monolayer $MoS_2$ field-effect transistor based dna sensors for screening of down syndrome, Nano Lett. 19 (2019) 1437–1444.

[18] J.R. Brent, N. Savjani, P. O'Brien, Synthetic approaches to two-dimensional transition metal dichalcogenide nanosheets, Prog. Mater. Sci. 89 (2017) 411–478.

[19] L. Yuwen, H. Yu, X. Yang, J. Zhou, Q. Zhang, Y. Zhang, Z. Luo, S. Su, L. Wang, Rapid preparation of single-layer transition metal dichalcogenide nanosheets via ultrasonication enhanced lithium intercalation, Chem. Commun. 52 (2016) 529–532.

[20] G. Guan, S. Zhang, S. Liu, Y. Cai, M. Low, C.P. Teng, I.Y. Phang, Y. Cheng, K.L. Duei, B.M. Srinivasan, Y. Zheng, Y.W. Zhang, M.Y. Han, Protein induces layer-by-layer exfoliation of transition metal dichalcogenides, J. Am. Chem. Soc. 137 (2015) 6152–6155.

[21] X. Huang, Z. Zeng, H. Zhang, Metal dichalcogenide nanosheets: preparation, properties and applications, Chem. Soc. Rev. 42 (2013) 1934–1946.

[22] L. Cheng, J. Liu, X. Gu, H. Gong, X. Shi, T. Liu, C. Wang, X. Wang, G. Liu, H. Xing, W. Bu, B. Sun, Z. Liu, PEGylated $WS_2$ nanosheets as a multifunctional theranostic agent for in vivo dual-modal CT/photoacoustic imaging guided photothermal therapy, Adv. Mater. 26 (2014) 1886–1893.

[23] Y. Yuan, R. Li, Z. Liu, Establishing water-soluble layered $WS_2$ nanosheet as a platform for biosensing, Anal. Chem. 86 (2014) 3610–3615.

[24] J.D. Qiu, H.Z. Peng, R.P. Liang, J. Li, X.H. Xia, Synthesis, characterization, and immobilization of prussian blue-modified Au nanoparticles: application to electrocatalytic reduction of $H_2O_2$, Langmuir 23 (2007) 2133–2137.

[25] A. Shah, R. Qureshi, N.K. Janjua, S. Haque, S. Ahmad, Electrochemical and spectroscopic investigations of protonated ferrocene-DNA intercalation, Anal. Sci. 24 (2008) 1437–1441.

[26] P. Liu, X.H. Yang, S. Sun, Q. Wang, K.M. Wang, J. Huang, J.B. Liu, L.L. He, Enzyme-free colorimetric detection of DNA by using gold nanoparticles and hybridization chain reaction amplification, Anal. Chem. 85 (2013) 7689–7695.

[27] R. Laocharoensuk, Development of electrochemical immunosensors towards point-of-care cancer diagnostics: clinically relevant studies, Electroanalysis 28 (2016) 1716–1729.

Please cite this article as: G. Hong et al., One-pot ultrasonic synthesis of multifunctional Au nanoparticle-ferrocene-$WS_2$ nanosheet composite for the construction of an electrochemical biosensing platform, Analytica Chimica Acta, https://doi.org/10.1016/j.aca.2019.11.038

[28] Y. Chen, K. Wang, Z. Liu, R. Sun, D. Cui, J. He, Rapid detection and quantification of tumor marker carbohydrate antigen 72-4 (CA72-4) using a superparamagnetic immunochromatographic strip, Anal. Bioanal. Chem. 408 (2016) 2319–2327.

[29] D. Wu, Z. Guo, Y. Liu, A. Guo, W. Lou, D. Fan, Q. Wei, Sandwich-type electrochemical immunosensor using dumbbell-like nanoparticles for the determination of gastric cancer biomarker CA72-4, Talanta 134 (2015) 305–309.

[30] H. Fan, Z. Guo, L. Gao, Y. Zhang, D. Fan, G. Ji, B. Du, Q. Wei, Ultrasensitive electrochemical immunosensor for carbohydrate antigen 72-4 based on dual signal amplification strategy of nanoporous gold and polyaniline–Au asymmetric multicomponent nanoparticles, Biosens. Bioelectron. 64 (2015) 51–56.

Please cite this article as: G. Hong et al., One-pot ultrasonic synthesis of multifunctional Au nanoparticle-ferrocene-$WS_2$ nanosheet composite for the construction of an electrochemical biosensing platform, Analytica Chimica Acta, https://doi.org/10.1016/j.aca.2019.11.038